Frequency doubling broadband light in multiple crystals

W. J. Alford and A. V. Smith

Dept. 1118 Lasers, Optics and Remote Sensing, Sandia National Laboratories, Albuquerque, NM 87185-1423

Abstract

We compare frequency doubling of broadband light in a single nonlinear crystal with doubling in five crystals with intercrystal temporal walk off compensation, and with doubling in five crystals adjusted for offset phase matching frequencies. Using a plane-wave, dispersive numerical model of frequency doubling we study the bandwidth of the second harmonic and the conversion efficiency as functions of crystal length and fundamental irradiance. For low irradiance the offset phase matching arrangement has lower efficiency than a single crystal of the same total length but gives a broader second harmonic bandwidth. The walk off compensated arrangement gives both higher conversion efficiency and broader bandwidth than a single crystal. At high irradiance, both multicrystal arrangements improve on the single crystal efficiency while maintaining broad bandwidth.

1. INTRODUCTION

Sometimes it is necessary to frequency mix broadband light in nonlinear crystals. If the broad bandwidth is associated with short, transform limited pulses this mixing process is well understood. However, there are few systematic studies of nonlinear mixing of multiple-longitudinal-mode, or broadband, light. That is the subject of this paper. In single-crystal mixing the conversion efficiency suffers and the bandwidth of the generated light narrows if the group-velocity walk off between input and output waves exceeds the inverse of the

DISCLAIMER

input bandwidth. In other words, when the crystal acceptance bandwidth is less than the bandwidth of the input light. One suggested method for improving the mixing efficiency and also increasing the output bandwidth is to use multiple short crystals with their phase matching wavelengths spread across the bandwidth of the input light. In this distributed Δk (DDK) arrangement, each crystal phase matches a different portion of the spectrum[1–4]. A second approach is to compensate for group velocity walk off between multiple short crystals[5,6]. This walk off compensated (WOC) arrangement effectively increases the acceptance bandwidth relative to a single crystal of the same total length by a factor equal to the number of crystals. A third approach is to angularly disperse the broadband fundamental light so each spectral component propagates at its phase matching angle in a critically phase matched crystal[7]. In the context of femtosecond mixing this is often referred to as tilted wavefront mixing[8,9]. It relies on the combination of lateral walk off and tilted wavefronts to match the group velocities of the short pulses. This group velocity matched (GVM) mixing is sometimes based on noncollinear phase matching. Equalizing the fundamental and harmonic group velocities maximizes the effective acceptance bandwidth and efficiency.

All of these multicrystal schemes can be evaluated analytically in the low conversion, plane wave limit. However, for strongly driven mixing a numerical model is essential. In this paper we use the numerical model of broadband mixing described in an earlier paper[10] (called method #1 in that paper). We are interested in the case where the light's bandwidth is much greater than the transform of the pulse duration. In other words, there is structure in the optical fields with a time scale much shorter than the pulse duration. We numerically construct such pulses by combining multiple longitudinal modes, giving them a Gaussian amplitude distribution and a random phase distribution. This chaotic light stream is then multiplied by a Gaussian time profile to simulate a nanosecond scale pulse from a multimode Q-switched laser. We numerically integrate a set of mixing equations that incorporate both group velocity and group velocity dispersion but not diffraction or birefringent walk off[10]. We perform the integration using a split-step technique in which propagation is handled by fast Fourier methods while nonlinear interaction is handled using Runge-Kutta integration.

As a concrete example we have chosen type I second-harmonic generation of a 420 nm, 1 ns (FWHM) pulse with 419 GHz bandwidth (FWHM) in a chain of five BBO crystals or in a single crystal. The relevant properties of BBO are listed in table I. This choice of second harmonic generation allows us to simplify our discussions, but many of our results can be extended to other three-wave mixing processes, and our model is applicable to any such process. In the following sections we will discuss first weakly driven, or low conversion mixing then follow with a discussion of strongly driven mixing.

2. WEAKLY DRIVEN DOUBLING

Many of the properties of broadband frequency doubling can be derived analytically in the limit of low conversion efficiency. For our example we construct a chaotic fundamental field by filling a set of longitudinal modes using a Gaussian distribution of amplitudes and a random set of phases. The pulse length is 1 ns and the longitudinal mode separation is 500 MHz. We use 1600 modes so the spectrum is uniformly filled from - 400 GHz to 400 GHz. We then multiply this spectrum by a Gaussian envelope with width 419 GHz. This chaotic light is strongly amplitude modulated and is a reasonable simulation of a broadband Q-switched laser. It is comprised of a train of spikes with more or less random phase and amplitude. The duration of the spikes is approximately the inverse of the bandwidth which for our 419 GHz fundamental bandwidth is about 2 ps. Temporal walk off between the fundamental and harmonic is 1.2 ps/mm due to their differing group velocities, so walk off is important for crystals thicker than 100 μm.

As a starting point for our discussion, we consider frequency doubling a single, 1 ps (FWHM) long, transform limited pulse in a single 10 mm long crystal. Our discussion is for plane waves only but we use irradiance levels corresponding to the center of a Gaussian profile of diameter 0.6 mm for added realism. Figure 1 shows results of a numerical simulation. The fundamental pulse is almost unchanged after passage through the crystal because we have chosen a fundamental energy low enough to keep mixing efficiency low. Because of its

slower group velocity the second harmonic pulse is stretched in time to about 12 ps, the temporal walk off between fundamental and harmonic. The leading edge of this stretched harmonic pulse is generated near the crystal's exit face, while the trailing edge is generated near its entrance face. Each part of the fundamental field can be considered to generate a 12 ps long square pulse of harmonic field, so the total harmonic field can be constructed by adding all these contributions. This summation yields the expression

$$\varepsilon_{\text{Harm}}(t') = \kappa \int dt \varepsilon^2_{\text{Fund}}(t'-t) S_\tau(t)/\tau, \tag{1}$$

where $S_\tau(t)$ is a square topped function with width equal to the group velocity walk off, τ,

$$S_\tau(t) = \begin{cases} 1 \text{ for } |t| < (\tau/2) \\ 0 \text{ for } |t| > (\tau/2), \end{cases} \tag{2}$$

and κ is a constant accounting for the nonlinear coefficient, the frequencies, and the refractive indices. Thus the harmonic field is a convolution of the square of the fundamental field and $S_\tau(t)$. The harmonic spectrum,$\mathcal{S}_{\text{Harm}}(\omega)$, is the Fourier transform of the harmonic field, and the transform of a convolution is the product of transforms for the two convolved functions, so

$$\mathcal{S}_{\text{Harm}}(\omega) = \mathcal{F}\{\varepsilon^2_{\text{Fund}}(t)\}\mathcal{F}\{S_\tau(t)/\tau\}, \tag{3}$$

where $\mathcal{F}\{\}$ represents a Fourier transform. The transform of the square function is a sinc function,

$$\mathcal{F}\{S_\tau(t)/\tau\} = \sqrt{\frac{1}{2\pi}}\,\text{sinc}(\Delta\omega\tau/2). \tag{4}$$

We will refer to the sinc function as the envelope function throughout the remainder of the paper. In our example, $\mathcal{F}\{\varepsilon^2_{\text{Fund}}(t)\}$ is a Gaussian of width (FWHM) 440 GHz, while

$$\mathcal{F}\{S_{12\,\text{ps}}(t)/12\text{ps}\} = \sqrt{\frac{1}{2\pi}}\text{sinc}(6\text{ps}\Delta\omega). \tag{5}$$

This sinc function has its first nulls at $\nu = \pm 1/(12\,\text{ps}) = \pm 83$ GHz, so its width is twice the fundamental acceptance bandwidth of 42 GHz for a 10 mm crystal (see table I). Figure 2 shows the power spectra for the fundamental and second harmonic, the latter being $|\mathcal{S}_{\text{Harm}}(\omega)|^2$.

As is well known, scanning a monochromatic laser across the phase matched wavelength of a second harmonic generation crystal produces second harmonic with power proportional to $\mathrm{sinc}^2(\Delta kL/2)$, where $\Delta k = k_{2\omega} - 2k_\omega$. Using the relationship between the group velocities, v_ω, and Δk

$$\frac{1}{v_\omega} = \frac{dk_\omega}{d\omega} \tag{6}$$

we see that Δk is related to the detuning of the second harmonic from phase matching, $\Delta\omega$, by

$$\Delta k = \frac{dk_{2\omega}}{d\omega}\Delta\omega - \frac{dk_\omega}{d\omega}\Delta\omega = \left(\frac{1}{v_{2\omega}} - \frac{1}{v_\omega}\right)\Delta\omega, \tag{7}$$

so

$$\mathrm{sinc}(\Delta kL/2) = \mathrm{sinc}(\tau\Delta\omega/2). \tag{8}$$

Thus the envelope function can be measured by scanning a monochromatic laser across the phase matching point.

The second harmonic fluence, f_{Harm} can be found by integrating the spectral power over frequency

$$f_{\mathrm{Harm}} \propto \int d(\Delta\omega)|\mathcal{S}(\Delta\omega)|^2. \tag{9}$$

According to Eq. (3), the fluence is proportional to the spectral integral of the product of the power spectrum of the fundamental field squared and the envelope function squared. If we could reduce the group velocity walk off, τ, the envelope function would broaden in $\Delta\omega$ while maintaining its amplitude. According to Eq. (9), this would give a higher doubling efficiency. This reflects the fact that the quantity $\int dt\varepsilon_{\mathrm{Harm}}(t)$ would be constant, independent of the walk off time, but the quantity $\int dt|\varepsilon_{\mathrm{Harm}}(t)|^2$ would increase, boosting the second harmonic fluence.

Note that although in the regime of low conversion efficiency the second harmonic spectrum is narrowed by temporal walk off and the efficiency falls by approximately the ratio

of the harmonic to fundamental spectral width, this does not mean that only the spectral center of the fundamental wave is depleted, nor that the conversion efficiency is limited by the crystal's acceptance bandwidth. In fact numerical simulation shows that the conversion efficiency can exceed 90% with little distortion of the fundamental spectrum. Additionally, the harmonic spectrum changes relatively little, with the most noticeable change being that the secondary peak structure washes out. These claims can be verified using the function PW-mix-SP in the nonlinear optics software SNLO[12].

A. SINGLE CRYSTAL

From this understanding of short pulse doubling we can predict the characteristics of broadband doubling in a single crystal. Each spike in the chaotic light generates a trailing, nearly square pulse of harmonic just like a solitary short pulse does. These overlap and interfere but the resulting harmonic wave can once again be constructed as a convolution of the square of the fundamental field with the square topped function of length equal to the walk off. As before the harmonic spectrum is $|\mathcal{F}\{\varepsilon^2_{\text{Fund}}(t)\}\mathcal{F}\{(S_\tau(t)/\tau\}|^2$, but for broadband light $\mathcal{F}\{\varepsilon^2_{\text{Fund}}(t)\}$ is highly structured, reflecting the chaotic nature of the fundamental wave. The envelope of the spectrum is still $[\text{sinc}^2(\Delta\omega\tau/2)/\sqrt{2\pi}]$ implying that the width of the second harmonic spectrum will be nearly the same as for the single, 1 ps pulse even though the harmonic pulse length is now about 700 ps rather than 12 ps. Figure 3 shows an example of such a spectrum, computed using our numerical model. In the top trace (Fig. 3(a)) we show the harmonic spectrum assuming the fundamental and harmonic waves have identical group velocities (GVM). This is $|\mathcal{F}\{\varepsilon^2_{\text{Fund}}(t)\}|^2$. The next trace (Fig. 3(b)) is for a temporal walk off of 12 ps. This is $|\mathcal{F}\{\varepsilon^2_{\text{Fund}}(t)\}|^2|\mathcal{F}\{S_{12}(t)/12\,\text{ps}\}|^2$, so we expect the same spectral fine structure but with different envelopes. In Fig. 4 we show a view of these spectra expanded about zero offset. Clearly the fine structure in the spectra are similar, as expected. The relative second harmonic powers for the cases with and without walk off is given by the ratio of their integrated spectral powers $\int d(\Delta\omega)|\mathcal{S}(\Delta\omega)|^2$. With walk off the power is re-

duced by approximately the ratio of the acceptance bandwidth to the fundamental spectral bandwidth.

An alternative method of estimating the relative powers is to compare both cases to doubling a 1 ns, single-longitudinal-mode (SLM) pulse. The harmonic field at any time point is comprised of a sum of contributions from the fundamental over the preceding 12 ps. In the single mode case these contributions add constructively since they all have the same phase, and they all have nearly the same amplitude because the fundamental amplitude variation over 12 ps is quite small. For our example, the doubling efficiency for the single mode case is 1.3%. For the chaotic case with no walk off we expect the efficiency to be twice as great, 2.6%, reflecting the well known factor of 2 improvement for multimode light relative to single mode light. This is due to the spikey nature of chaotic light. Most of the energy is contained in amplitude spikes of duration approximately 2 ps for our bandwidth of 419 GHz. Our numerical model yields the expected 2.6% efficiency for zero walk off. If we add walk off there are about 6 uncorrelated contributions to the harmonic field at each point, reflecting the 2 ps coherence time and the 12 ps walk off time. This implies that the net harmonic field should be reduced by a factor of about $\sqrt{6}$. Squaring this to obtain an irradiance gives a reduction of roughly 6 relative to the zero walk off case, or 3 relative to the single-mode case. The numerical model gives a slightly larger reduction of 3.7. The incoherent summation also means that the efficiency scales linearly with crystal length for chaotic light rather than quadratically as is characteristic of single mode light. Another way of saying this is that the chaotic efficiency is reduced by the ratio of the crystal acceptance bandwidth to the light bandwidth. However, just as in the case of doubling the 1 ps pulse, this does not mean that only the central portion of the fundamental spectrum is converted. The full fundamental spectrum contributes and is universally depleted.

B. MULTIPLE CRYSTALS WITH WALK OFF COMPENSATION

The effects of temporal walk off can be reduced by reversing the walk off between mixing crystals. For wavelengths longer than those of our example the birefringence of BBO can be used[6] to compensate walk off, but we admit that for 420 nm doubling we know of no crystal with sufficient birefringence. Ignoring this practical difficulty, if we reconsider the doubling of a 1 ps pulse, walk off compensation (WOC) would reduce the width of the second harmonic pulse from 12 ps to about 3 ps, the convolution of the 1 ps pulse and a 2.4 ps (=12 ps/5) square pulse. The harmonic field would be correspondingly stronger by a factor of 4 or so. Irradiance would be 16 times higher but duration would be 4 times smaller implying a conversion efficiency 4 times higher than for the single 10 mm crystal. The shorter duration also translates to a broader harmonic spectrum. More quantitatively, the square topped convolution function has a width of 2.4 ps so the envelope function is

$$\mathcal{F}\{S_{2.4\mathrm{ps}}(t)/2.4\mathrm{ps}\} = \sqrt{\frac{1}{2\pi}}\mathrm{sinc}(1.2\mathrm{ps}\Delta\omega). \tag{10}$$

Its peak height is unchanged but its width is 5 times that of the uncompensated case with the same total crystal length.

For a chaotic fundamental field the harmonic field is again the convolution of the square of the fundamental field with the 2.4 ps wide square pulse. The first nulls of the sinc envelope should lie at ±420 GHz. This is illustrated in the model-generated spectrum shown in Fig. 3(c). Figure 4(c) shows that the structure at the center of the spectrum is again $|\mathcal{F}\{\varepsilon^2_{\mathrm{Fund}}(t)\}|^2$, unchanged by walk off compensation.

Walk off compensation means that each time point in the second harmonic pulse receives contributions from the preceding 2.4 ps of fundamental, rather than the preceding 12 ps. The number of uncorrelated contributions is thus about 1.2 rather than 6. Further, each point receives equal contributions from each of the 5 crystals. Taken together these effects should increase the efficiency relative to the uncompensated chaotic case by a factor of nearly 5. The actual enhancement in our example is 4.0. We conclude that walk off compensation

in 5 crystals improves the chaotic light doubling efficiency by a factor of 4 in our example compared with a single 10 mm long crystal. The higher efficiency is associated with a factor of 5 broadening of the envelope function.

C. MULTIPLE CRYSTALS WITH OFFSET Δk's

An alternative method of broadening the spectrum of doubled chaotic light is to use multiple crystals each adjusted to phase match a different portion of the fundamental spectrum (DDK). This is a misleading description of the doubling process since, as we have stated, frequency doubling depletes the entire fundamental spectrum even though the harmonic spectrum is narrowed to the crystal's acceptance bandwidth. Returning to the 1 ps pulse, if a crystal has nonzero phase velocity mismatch, ($\Delta k \neq 0$), the contributions to the harmonic pulse from different positions in the crystal have different phases, so the square pulse, $S_\tau(t)$, is replaced by $S_\tau(t)\exp(i\Delta kLt/\tau)$. The Fourier transform of this is a sinc function centered at $\omega_0 = -(\Delta kL)/\tau$. So the spectrum is $|G_{440}(\Delta\omega)|^2|\mathrm{sinc}(\tau\Delta\omega + \Delta kL/\tau)|^2$ where $G_{440}(\Delta\omega)$ is a Gaussian of width 440 GHz, the transform of the 1 ps Gaussian fundamental pulse. If the single 10 mm crystal in our example is replaced by five crystals, each 2 mm long, and each with different phase mismatch, Δk, the function $S_\tau \exp(i\Delta kLt/\tau)$ is replaced by a sequence of 5 square pulses, each 2.4 ps long, and each with a phase chirp, or frequency offset of $\omega_0 = -(\Delta k 2\mathrm{mm})/(2.4\mathrm{ps})$ appropriate to its individual value of Δk. The phases of these square pulses are adjusted so they splice together without phase discontinuities. The envelope function is then the Fourier transform of this 12 ps long square topped pulse that has 5 zones with different phase chirps. A reasonable spacing of the phase matching centers is half the acceptance bandwidth for a 2 mm crystal, or 5.5 cm^{-1}. This set of Δk's can be sequenced in 30 distinct orders, but only those with offsets sequenced red to blue or vice versa produce an envelope function without deep interference dips near line center. This envelope function is shown in Fig. 5. It is about 5 times wider than for the single crystal but also about 10 times lower in maximum value. We verified that the numerical model

gives this envelope function by dividing the model-generated DDK harmonic spectrum by the corresponding GVM spectrum. Envelope functions for other crystal sequences have the same area but tend to be more spread in frequency with deep interference dips. The product of the envelope function with $|\mathcal{F}\{\varepsilon^2_{\text{Fund}}(t)\}|^2$ is shown in Fig. 3(d) and expanded in Fig. 4(d). The doubling efficiency for our example is 0.21%, less than for the group velocity matched case (GVM)(2.6%), the single crystal with walk off (SCW)(0.35%), or the walk off compensated crystals (WOC)(1.4%).

As we showed above, tuning monochromatic fundamental light across the phase matched zone also maps out the envelope function. That is the analysis approach of Brown[1] and of Babushkin *et al.*[2]. Brown used a plane-wave, monochromatic model to compute the conversion versus frequency in 6 crystals with detunings approximately equal to an acceptance bandwidth. She also tested this experimentally by doubling 250 ns pulses of broadband 972 nm light in 6 type I BBO crystals, each of length 2.5 mm. The second harmonic was then doubled to 243 nm in another set of 6 type I BBO crystals. She verified the expanded spectrum of the 243 nm light relative to that expected for a single crystal of the same length. However, she did not compare the efficiency of these two methods. Babushkin *et al.* did similar experiments using two type II KDP crystals to sum single-mode, 100 ps pulses of 532 and 1064 nm light. The crystal lengths were 9 and 16 mm. They used beam tilt to simulate frequency tuning and mapped envelope functions for fixed crystal angles but with varying intercrystal phase shifts.

D. SUMMARY OF WEAKLY DRIVEN DOUBLING

In weakly driven second harmonic generation the fundamental wave is altered little by doubling. We showed that in this case the second harmonic spectra is given by the product of the Fourier transform of the square of the fundamental field, $\mathcal{F}\{\varepsilon^2_{\text{Fund}}(t)\}$ and an envelope function that characterizes group velocity walk off and phase mismatch in the crystal or set of crystals. The former is the same for all arrangements so the envelope functions determine the

efficiencies since the conversion efficiency is directly proportional to the integrated spectral power. This makes it quite easy to calculate the doubling efficiency for broadband light relative to that for an otherwise identical monochromatic pulse. The envelope function can be calculated using the group velocity walk off and phase velocity mismatches for the crystals or it can be measured by scanning a monochromatic laser across the phase matching region.

We showed using a numerical model that the doubling efficiency for chaotic light is twice that of monochromatic light if the acceptance bandwidth of the crystal is much larger than the bandwidth of the chaotic light. When the bandwidth of the light is broad compared with the acceptance bandwidth, both the numerical model and our analytical calculations show that mixing in N crystals of length L/N with walk off compensation between them is equivalent to reducing the walk off by a factor of N and increasing the acceptance bandwidth by N. The doubling efficiency is improved by a comparable amount. Alternatively, the bandwidth of the second harmonic light can be increased by using several short crystals tilted so their phase matching wavelengths are distributed over the bandwidth of the broadband fundamental. The resulting efficiency is much less than for walk off compensation, and is less than for a single crystal. The shape of the envelope function for this arrangement is sensitive to the order of the phase mismatches with the preferred sequence being monotonic red to blue or blue to red.

The analysis methods described here are applicable to other mixing processes as long as the input waves have matched group velocities and the conversion is low. The input group velocities can sometimes be matched using noncollinear phasematching. Our analysis method is also applicable for mixing broadband light with single longitudinal mode light, whether the input group velocities are matched or not, so long as the pulse lengths are much greater than the temporal walk off.

3. STRONGLY DRIVEN DOUBLING

Our analysis of weakly driven doubling breaks down in the strongly driven case. It was based on the assumption that the fundamental wave is unaltered by doubling. In strong mixing the temporal and spectral structure of the fundamental can be drastically altered, in which case broadband doubling can only be accurately analyzed using numerical models with group velocity effects included, such as those of Milonni *et al.*[4], or Smith and Gehr[10]. In this section we present model results for the same cases discussed above except that the fundamental energy and the crystal lengths have been increased to reach the high conversion regime. We use the same chaotic fundamental light as before but scale up its energy. The damage fluence of BBO sets the upper limit on pulse energy.

Figure 6 shows second harmonic spectra for the same cases as before but with the fundamental input energy increased from 10 μJ to 10 mJ. The conversion efficiency for a single mode pulse is 98% under these conditions. For chaotic light but with no walk off, Fig. 6(a), the efficiency is 95%. The high resolution spectrum, shown in Fig. 7(a), is different from the low conversion case (Fig. 4(a)), but not by a large amount. Including walk off reduces the efficiency to 22% and dramatically changes the spectrum.

In Fig. 8 we plot conversion efficiency for a single crystal without walk off. As expected the efficiency approaches 100% with sufficient pulse energy and crystal length. Interestingly, the figure shows that even this case can be over driven. At high values of crystal length and pulse energy, the efficiency drops below its maximum. This is due to group velocity dispersion which changes the relative local phases of the fundamental and harmonic, allowing some back conversion from harmonic to fundamental. If the group velocity dispersions are set to zero, the hanging valley on the efficiency surface is raised to nearly 100%.

Fig. 9 is the same as Fig. 8 except we include walk off. The maximum conversion efficiency falls from almost 100% to about 30%. The shape of the harmonic spectral envelope shown in Fig. 6(b), is quite different from the weak doubling case. The side lobes have risen and the modulation has been washed out. This is to be contrasted with the profile traced

out by scanning a monochromatic laser across the phase matching region. At high doubling efficiency that produces a spectral shape with distinct side lobes but with a narrowed rather than broadened main peak[13], so scanning a single mode laser is not a useful measure of the harmonic envelope for strongly driven second harmonic generation.

Fig. 10 shows the efficiency surface for 5 walk off compensated crystals. There is a small zone where the efficiency is quite high, but as in the case of the single crystal it is possible to overdrive the crystals so the efficiency falls with increasing energy or crystal length. When this occurs the harmonic spectrum is also strongly modified, as shown in Fig. 7(c). From Figure 6(c) we see that the envelope function is now nearly square topped with side lobes.

Fig. 11 shows the efficiency surface for 5 crystals with distributed Δk's. This arrangement does not suffer from decreasing efficiency with increasing input energy within the range of the figure. The spectral envelope function (Fig. 6(d)) looks much like that at low efficiency (Fig. 3(d)) even though the spectral fine structure is highly altered (compare Figures 4(d) and 7(d)).

In Figure 12 we show doubling efficiency for a fixed total crystal length of 10.54 mm as the input energy varies. Individual curves correspond to a single crystal without walk off (GVM), a single crystal with walk off (SCW), 5 crystals with walk off compensation (WOC), and 5 crystals with distributed Δk's (DDK). Of the latter three, walk off compensation is 4 times as efficient at low energy. The distributed Δk arrangement is the least efficient at low energy but increases monotonically until it is the most efficient at the highest energy. Both the walk off compensated and single crystal cases show saturation, but the single crystal saturates at a lower energy. Bearing in mind that real beams have a transverse distribution of irradiance, in most cases the walk off compensated arrangement will give the highest efficiency unless the transverse profile is nearly square topped.

4. CONCLUSIONS

For weakly driven doubling, analysis of the spectra and conversion efficiency for the various crystal arrangements is straightforward. The harmonic spectrum is found by multiplying the Fourier transform of the square of the fundamental field by an envelope function determined by the temporal walk off and the crystal arrangement. In this regime, walk off compensation provides both high efficiency and a broad harmonic spectrum. Distributed Δk's also gives a broad spectrum but with reduced efficiency.

For strongly driven doubling, numerical modeling is essential for determining spectra and efficiencies. In this regime it is often possible to overdrive the crystals resulting in less than maximum conversion efficiency. The efficiency maxima for the various arrangements are 25% for a single crystal, 50% for walk off compensated crystals, and 50% for distributed Δk's. The most favorable arrangement is matched fundamental and harmonic group velocities. This can sometimes be achieved using noncollinear phase matching[7–9] at the cost of added complexity and perhaps limited interaction lengths. The efficiency can then approach 100%.

The type I doubling studied here is of limited generality in that the two input waves are identical and do not walk off from one another. If the input is two uncorrelated chaotic waves, the efficiency will be limited by photon imbalance in the two input beams, even in the absence of temporal walk off. The locally weaker input wave will be completely depleted some distance into the crystal. Past this point it will be regenerated with reversed phase. The stronger wave will also grow while the sum frequency wave will be depleted. In Fig. 13 we show mixing efficiency versus input energy for identical fundamental waves (filled dots), for uncorrelated chaotic input waves (filled squares), and for monochromatic pulses. Walk off in each case is zero but all other parameters are identical to our example case above. The uncorrelated efficiency is initially half that of the correlated case and identical to the monochromatic case, but saturates at an efficiency of about 30% due to photon imbalance.

We end with a reminder that for multiple crystals the relative signs of the effective nonlinear coefficient are important[14], as are the intercrystal phase shifts. Finally we recommend

the SNLO function PW-mix-BB[12] as a fast and simple approach to simulation of broadband mixing in a single crystal.

ACKNOWLEDGMENTS

This work was supported by the United States Department of Energy under contract DE-AC04-94AL85000. Sandia is a multiprogram laboratory operated by Sandia Corporation, a Lockheed Martin Company, for the United States Department of Energy.

REFERENCES

1. M. Brown, "Increased spectral bandwidths in nonlinear conversion processes by use of multicrystal designs," Opt. Lett. **23,** 1591-1593 (1998).

2. A. Babushkin, R. S. Craxton, S. Oskoui, M. J. Guardalben, R. L. Keck, and W. Seka, "Demonstration of the dual-tripler scheme for increased-bandwidth third-harmonic generation," Opt. Lett. **23,** 927-929 (1998).

3. D. Eimerl, J. M. Auerbach, C. E. Barker, D. Milam, and P. W. Milonni, "Multicrystal designs for efficient third-harmonic generation," Opt. Lett. **22,** 1208-1210 (1997).

4. P. W. Milonni, J. M. Auerbach, and D. Eimerl, "Frequency conversion modeling with spatially and temporally varying beams," SPIE vol. 2633 pp. 230-241 (1997).

5. A. V. Smith, D. J. Armstrong, and W. J. Alford, "Increased acceptance bandwidths in optical frequency conversion by use of multiple walk-off-compensating nonlinear crystals," J. Opt. Soc. Am. B **15,** 122-141 (1998).

6. R. J. Gehr, M. W. Kimmel, and A. V. Smith, "Simultaneous spatial and temporal walk-off compensation in frequency-doubling femtosecond pulses in β-BaB_2O_4," Opt. Lett. **23,** 1298-1300 (1998).

7. B. A. Richman, S. E. Bisson, R. Trebino, E. Sidick, and A. Jacobson, "Efficient broadband second-harmonic generation by dispersive achromatic nonlinear conversion using only prisms," Opt. Lett. **23,** 497-499 (1998).

8. R. Danielius, A. Piskarskas, P. Di Trapani, A. Andreoni, C. Solcia, and P. Foggi, "A collinearly phase-matched parametric generator/amplifier of visible femtosecond pulses," IEEE J. Quant. Electron. **34,** 459-463 (1998).

9. T. Wilhelm, J. Piel, and E. Riedle, "Sub-20-fs pulses tunable across the visible from a blue-pumped single-pass noncollinear parametric converter," Opt. Lett. **22,** 1494-1496 (1997).

10. A. V. Smith and R. J. Gehr, "Numerical models of broad-bandwidth nanosecond optical parametric oscillators," J. Opt. Soc. Am. B **16,** 609-619 (1999).

11. W. J. Alford, R. J. Gehr, R. L. Schmitt, A. V. Smith, and G. Arisholm, "Beam tilt and angular dispersion in broad-bandwidth, nanosecond optical parametric oscillators," J. Opt. Soc. Am. B **16,** 1525-1532 (1999).

12. Function 2D-mix-LP within SNLO. The SNLO nonlinear optics code is available from A. V. Smith.

13. See figures 15 and 16 of Ref. 5. See also M. A. Norton, D. Eimerl, C. A. Ebbers, S. P. Velsko, and C. S. Petty, "KD*P frequency doubler for high average power applications," in *Solid State Lasers*, Proc. SPIE **1223,** 75-83 (1990), and R. C. Eckardt and J. Reintjes, "Phase matching limitations of high efficiency second harmonic generation," IEEE J. Quantum Electron. **QE-20,** 1178-1187 (1984).

14. D. J. Armstrong, W. J. Alford, T. D. Raymond, A. V. Smith, and M. S. Bowers, "Parametric amplification and oscillation with walkoff-compensating crystals," J. Opt. Soc. Am. B **14,** 460-474 (1996).

FIGURES

Fig. 1. Normalized irradiance of the fundamental and second harmonic output from a 10 mm long BBO crystal in the low conversion regime. The input fundamental is a 1 ps (FWHM) Gaussian pulse. The second harmonic is stretched by 12 ps due to the group velocity difference between the fundamental and harmonic waves.

Fig. 2. Normalized spectra of the pulses of Figure 1. The fundamental is a Gaussian of width (FWHM) 440 GHz (14.7 cm^{-1}), the harmonic is the product of a Gaussian and a $|\mathrm{sinc}(\Delta\omega t)|^2$ function with its first nulls at $\pm$83 GHz (2.8 cm^{-1}).

Fig. 3. Low conversion efficiency normalized spectra of 210 nm second harmonic for a single crystal with matched fundamental and harmonic group velocities (GVM)(a), for a single crystal with actual BBO group velocity difference (SCW)(b), for 5 walk off compensated crystals (WOC) (c), and for 5 crystals with phase matched frequencies at $\Delta\omega$= -13.9, -6.94, 0, 6.94, 13.9 cm^{-1} (DDK)(d). The fundamental input energy is 10 μJ, resulting in a fluence of 2 mJ/cm^2. The fundamental has a FWHM bnadwidth of 419 GHz (14 cm^{-1}). The spectra are smoothed using a running average over 0.14 cm^{-1} to reduce the fine structure of the spectra for better readability. The spectrum of the input fundamental light is the same in each case.

Fig. 4. An expanded view of the spectra of Figure 3 showing that the harmonic spectra is similar in each case.

Fig. 5. The envelope function for 5 crystals with detunings $\Delta\omega$= -13.9, -6.94, 0, 6.94, 13.9 cm^{-1}.

Fig. 6. High converesion efficiency normalized harmonic spectra under the same conditions as Figure 3 except the fundamental pulse energy is increased from 10 μJ to 10 mJ.

Fig. 7. An expanded view of the spectra of Figure 6 showing that the harmonic spectra are significantly altered for strong doubling compared with weak doubling.

Fig. 8. Doubling efficiency versus crystal length and fundamental pulse energy for a crystal with no group velocity walk off (GVM).

Fig. 9. Doubling efficiency versus crystal length and fundamental pulse energy for a crystal with BBO's group velocity walk off (SCW).

Fig. 10. Doubling efficiency versus crystal length and fundamental pulse energy for 5 walk off compensated crystals (WOC).

Fig. 11. Doubling efficiency versus crystal length and fundamental pulse energy for 5 crystals with phase matching frequencies separated by half the crystal acceptance bandwidth (DDK).

Fig. 12. Doubling efficiency versus fundamental pulse energy for a total crystal length of 10.54 mm for a single crystal with no walk off (GVM)(solid dots), for a single crystal with walk off (SCW)(open dots), for 5 walk off compensated crystals (WOC)(squares), and for 5 crystals with phase matching frequencies separated by half the crystal acceptance bandwidth (DDK)(crosses).

Fig. 13. Doubling efficiency versus fundamental pulse energy for a total crystal length of 10.54 mm for a single crystal with no walk off (solid dots), for a single crystal with no walk off and uncorrelated chaotic inputs (open diamonds), and for a monochromatic input pulse (crosses).

TABLES

Table 1. Properties of BBO for doubling 420 nm light.

Property	420 nm		210 nm
Phase matching angle		76°	
Nonlinear coefficient		0.5 pm/V	
Polarization	ordinary		extraordinary
Refractive index	1.689		1.689
Group velocity	c/1.769		c/2.127
Group velocity dispersion	-1.07×10^5 cm/sec cm^{-1}		-3.16×10^5 cm/sec cm^{-1}
Temporal walk off (420-210 nm)		1.2 ps/mm	
Acceptance bandwidth		14 cm^{-1}-mm	

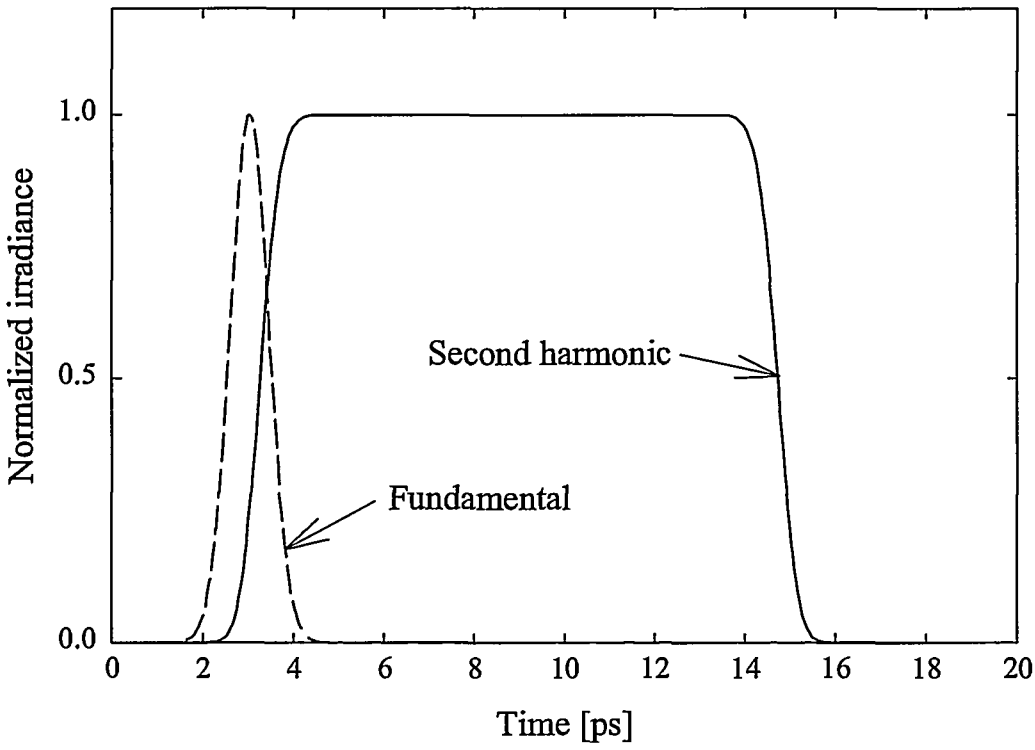
Normalized irradiance
1.0
0.5
0.0
0
2
4
6
8
10
12
14
16
18
20
Time [ps]
Second harmonic
Fundamental

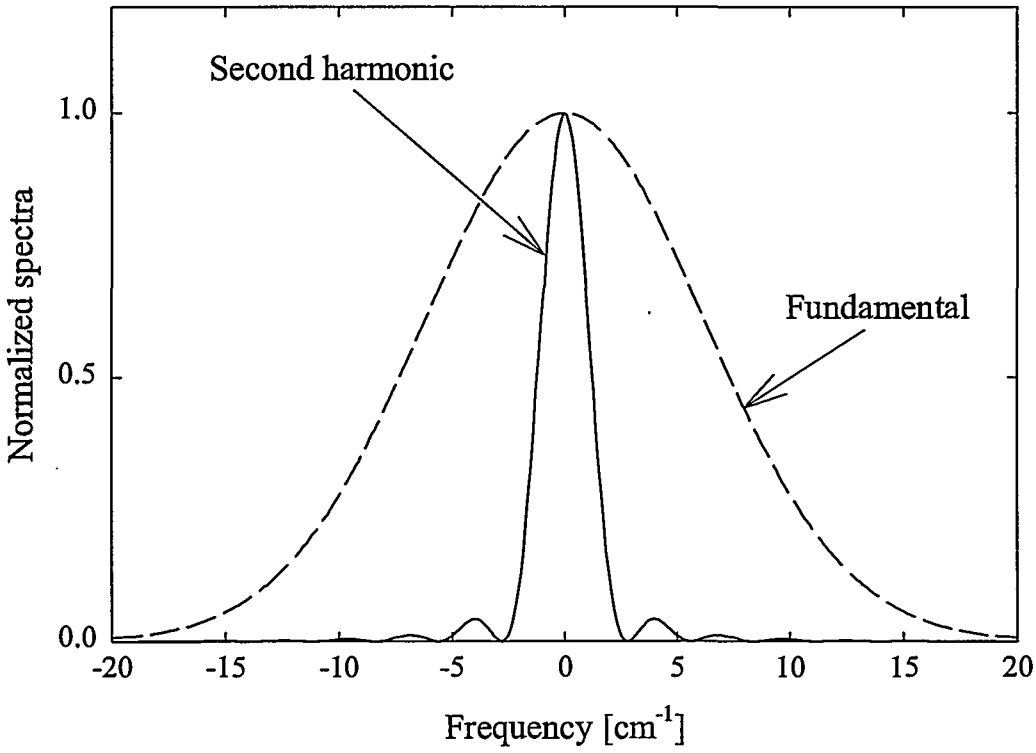
Second harmonic
Fundamental
Normalized spectra
1.0
0.5
0.0
-20
-15
-10
-5
0
5
10
15
20
Frequency [cm-1]

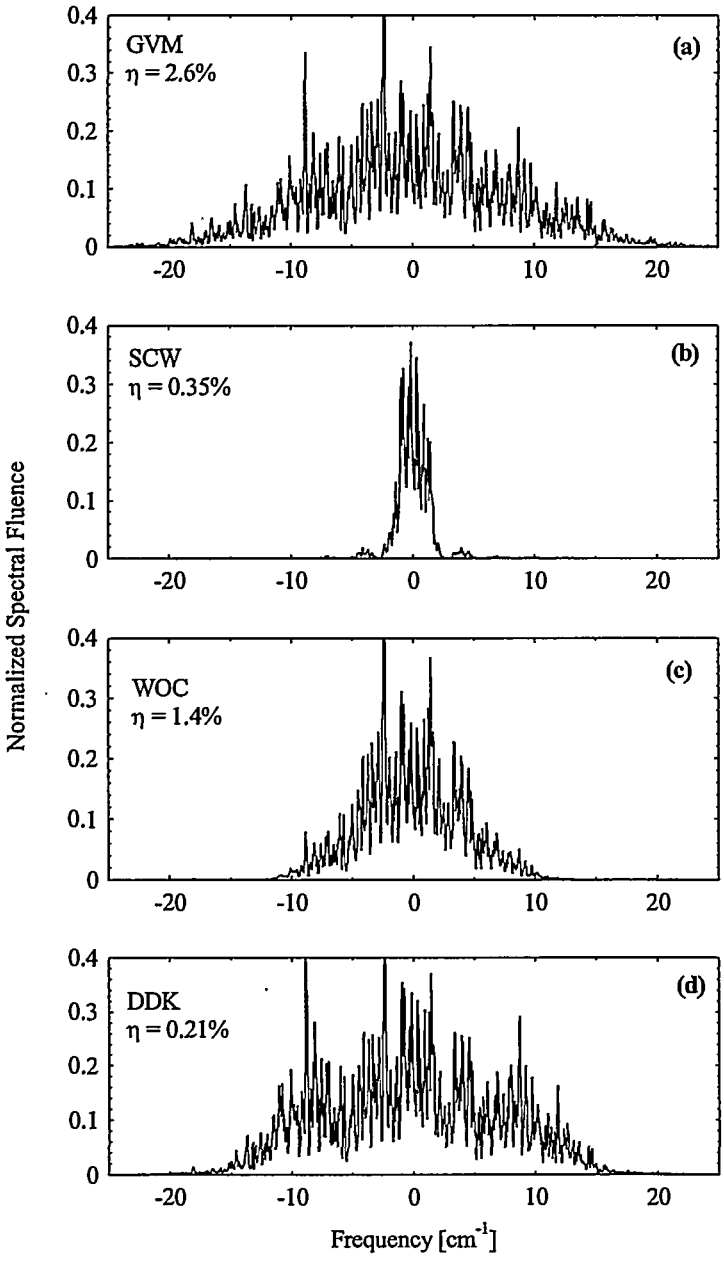
GVM
η = 2.6%
(a)
SCW
η = 0.35%
(b)
WOC
η = 1.4%
(c)
DDK
η = 0.21%
(d)
Normalized Spectral Fluence
Frequency [cm-1]
0.4
0.3
0.2
0.1
0
-20
-10
0
10
20

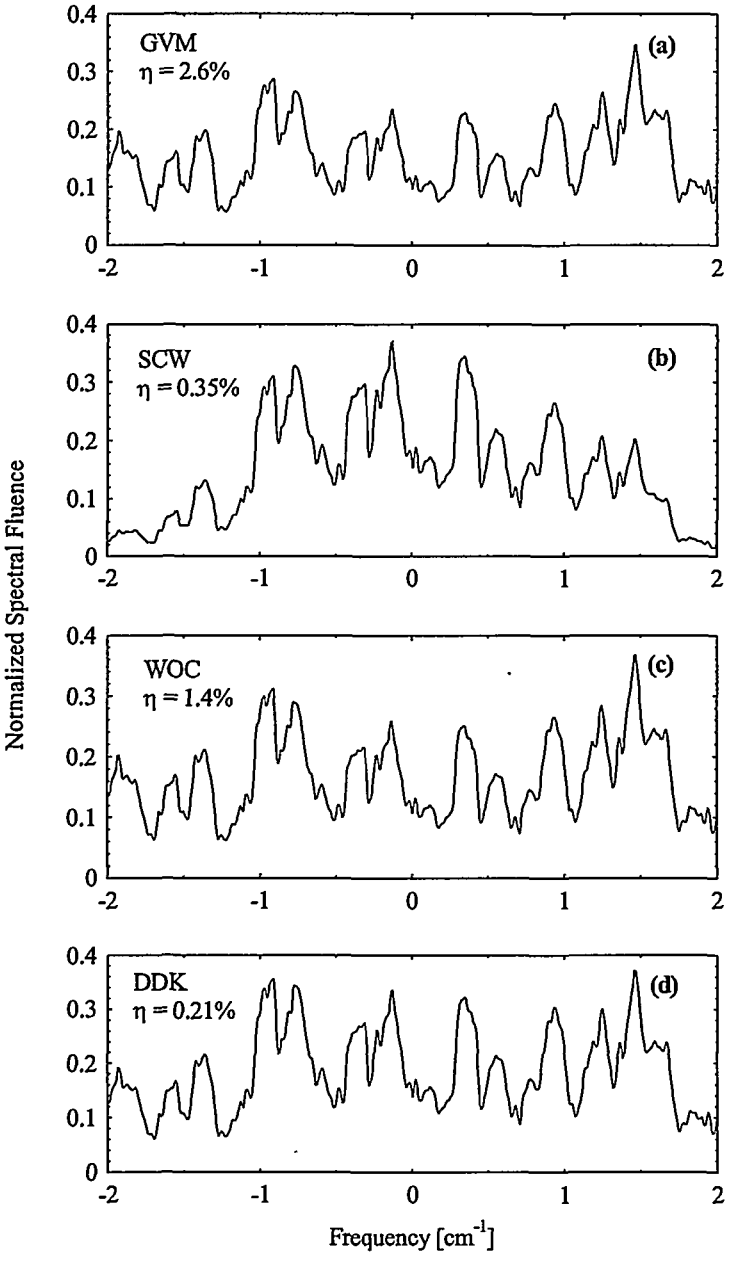
GVM
η = 2.6%
(a)
SCW
η = 0.35%
(b)
WOC
η = 1.4%
(c)
DDK
η = 0.21%
(d)
0.4
0.3
0.2
0.1
0
-2
-1
0
1
2
Normalized Spectral Fluence
Frequency [cm-1]

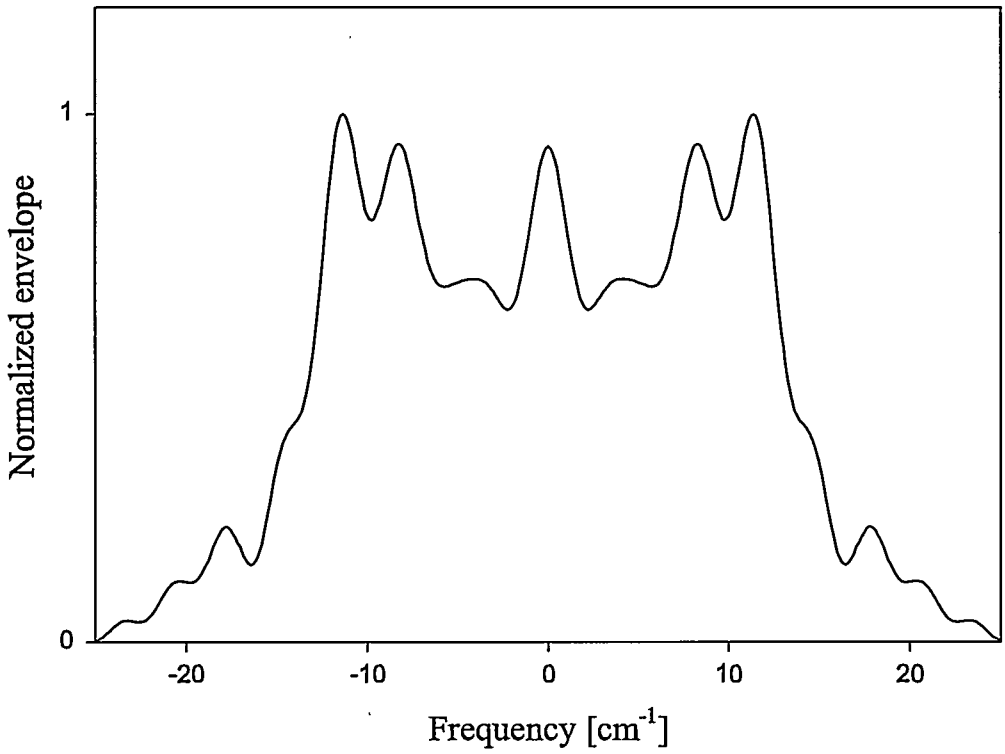
Normalized envelope
1
0
-20
-10
0
10
20
Frequency [cm-1]

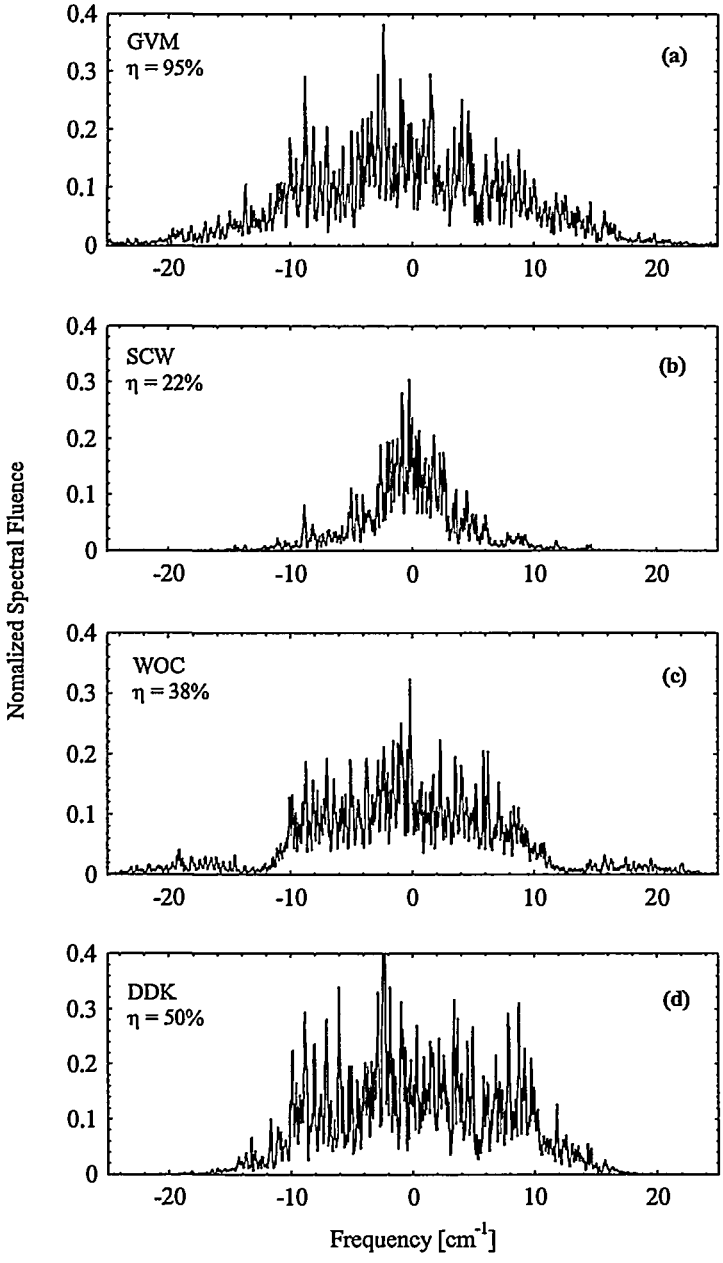
GVM
η = 95%
(a)
SCW
η = 22%
(b)
WOC
η = 38%
(c)
DDK
η = 50%
(d)
0.4
0.3
0.2
0.1
0
-20
-10
0
10
20
Nomalized Spectral Fluence
Frequency [cm-1]

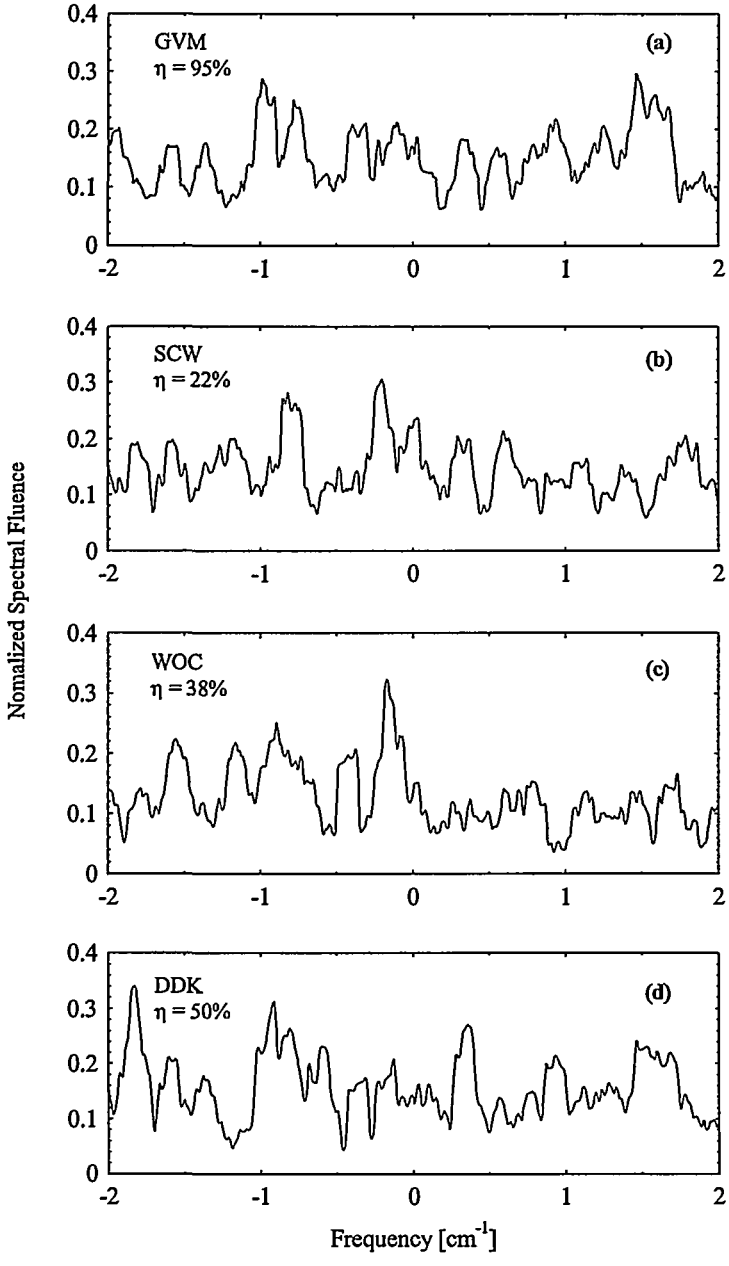
GVM
η = 95%
(a)
SCW
η = 22%
(b)
WOC
η = 38%
(c)
DDK
η = 50%
(d)
Nomalized Spectral Fluence
Frequency [cm-1]
0.4
0.3
0.2
0.1
0
-2
-1
0
1
2

GVM

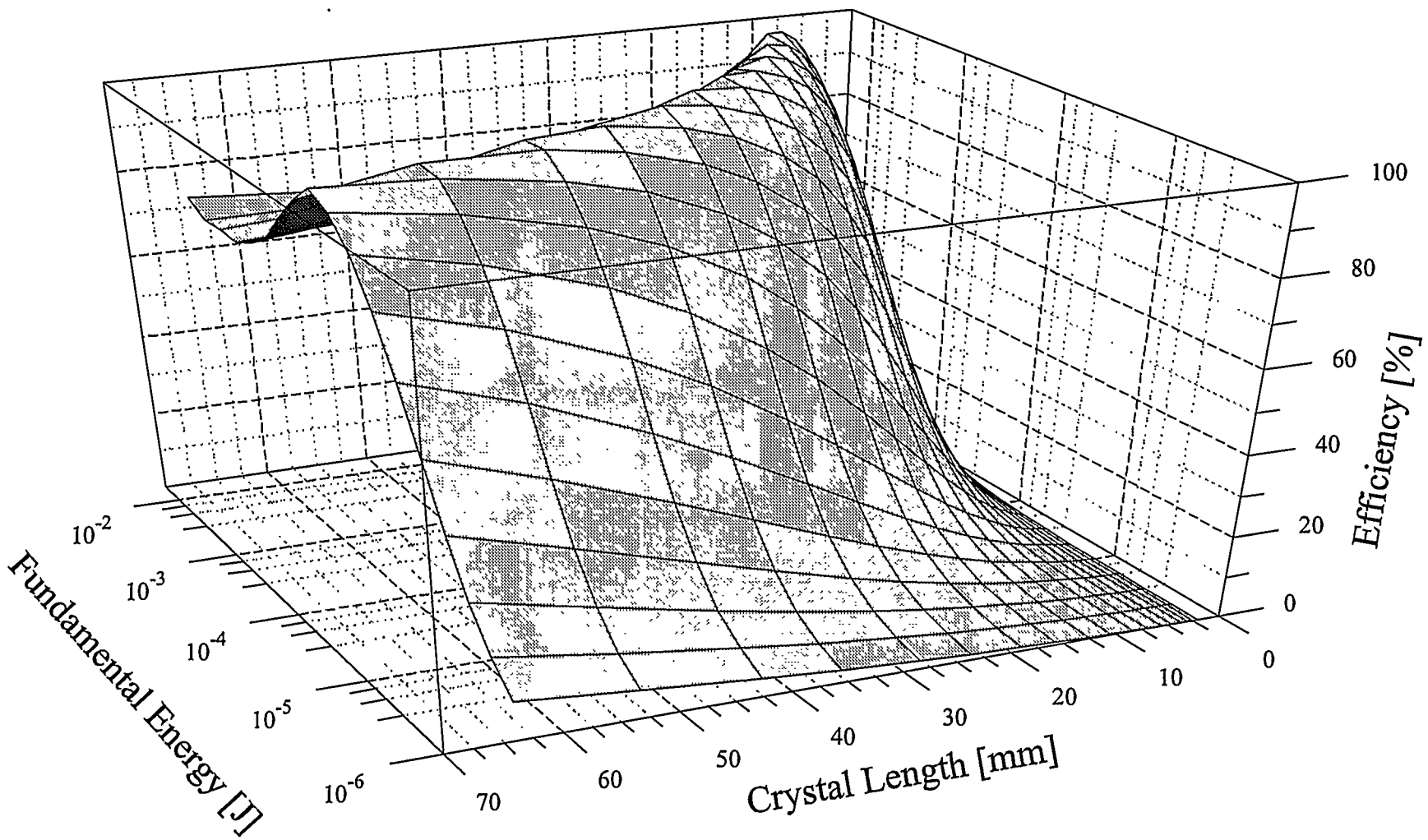
Fundamental Energy [J]
10^-2
10^-3
10^-4
10^-5
10^-6
Crystal Length [mm]
70
60
50
40
30
20
10
0
Efficiency [%]
100
80
60
40
20
0

SCW

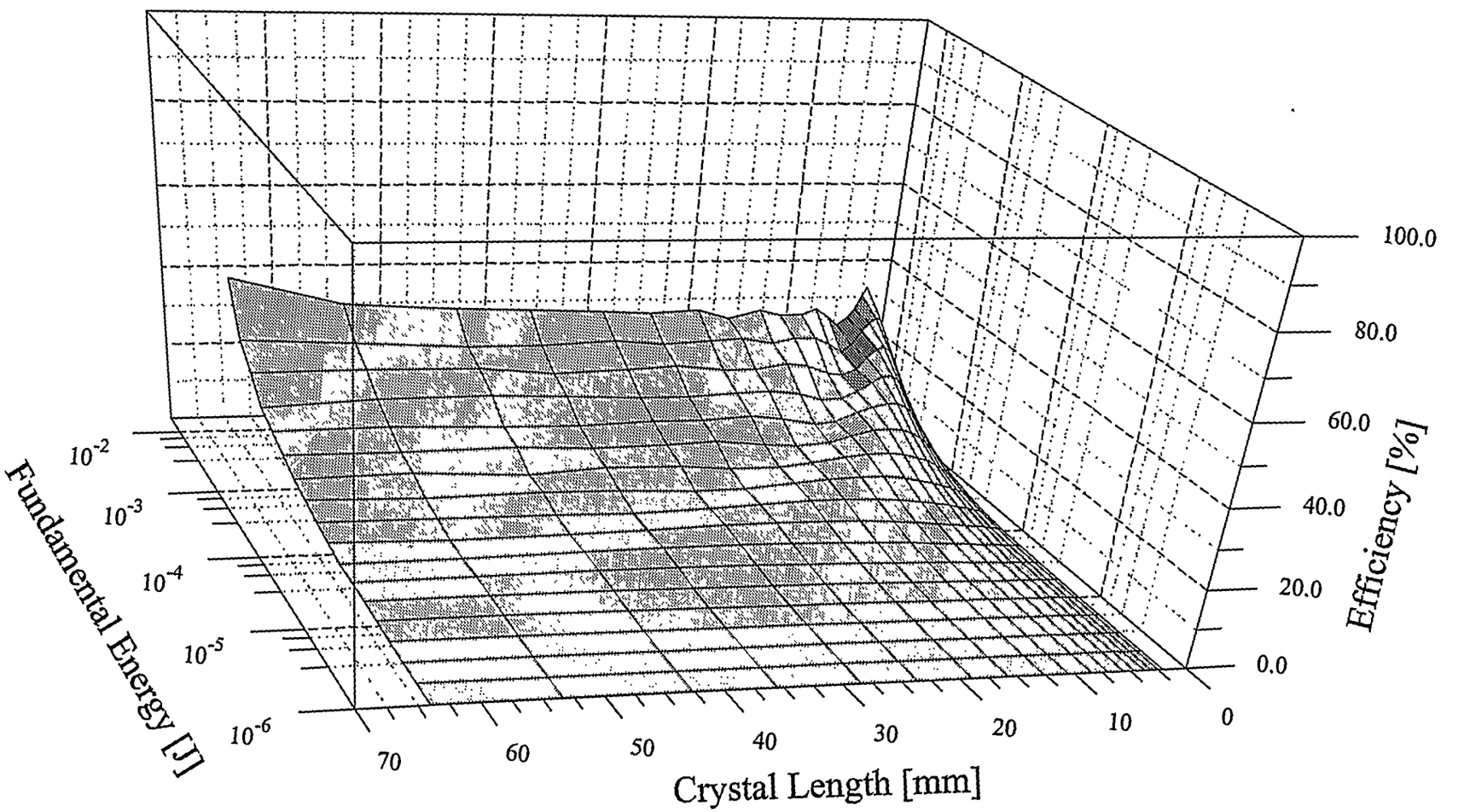
Fundamental Energy [J]
10^{-2}
10^{-3}
10^{-4}
10^{-5}
10^{-6}
70
60
50
40
30
20
10
0
Crystal Length [mm]
100.0
80.0
60.0
40.0
20.0
0.0
Efficiency [%]

WOC

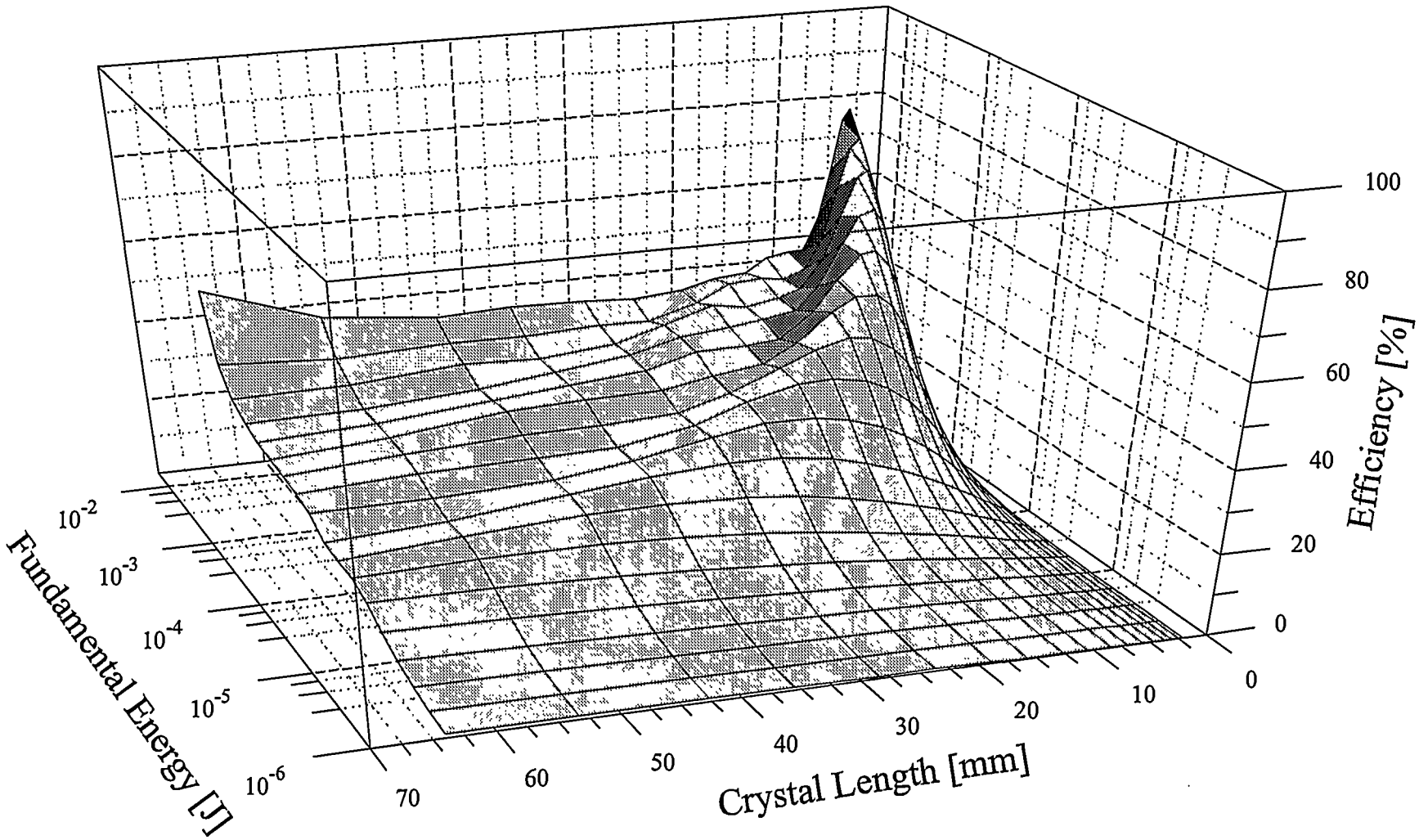
Fundamental Energy [J]
10^-2
10^-3
10^-4
10^-5
10^-6
Crystal Length [mm]
70
60
50
40
30
20
10
0
Efficiency [%]
100
80
60
40
20
0

DDK

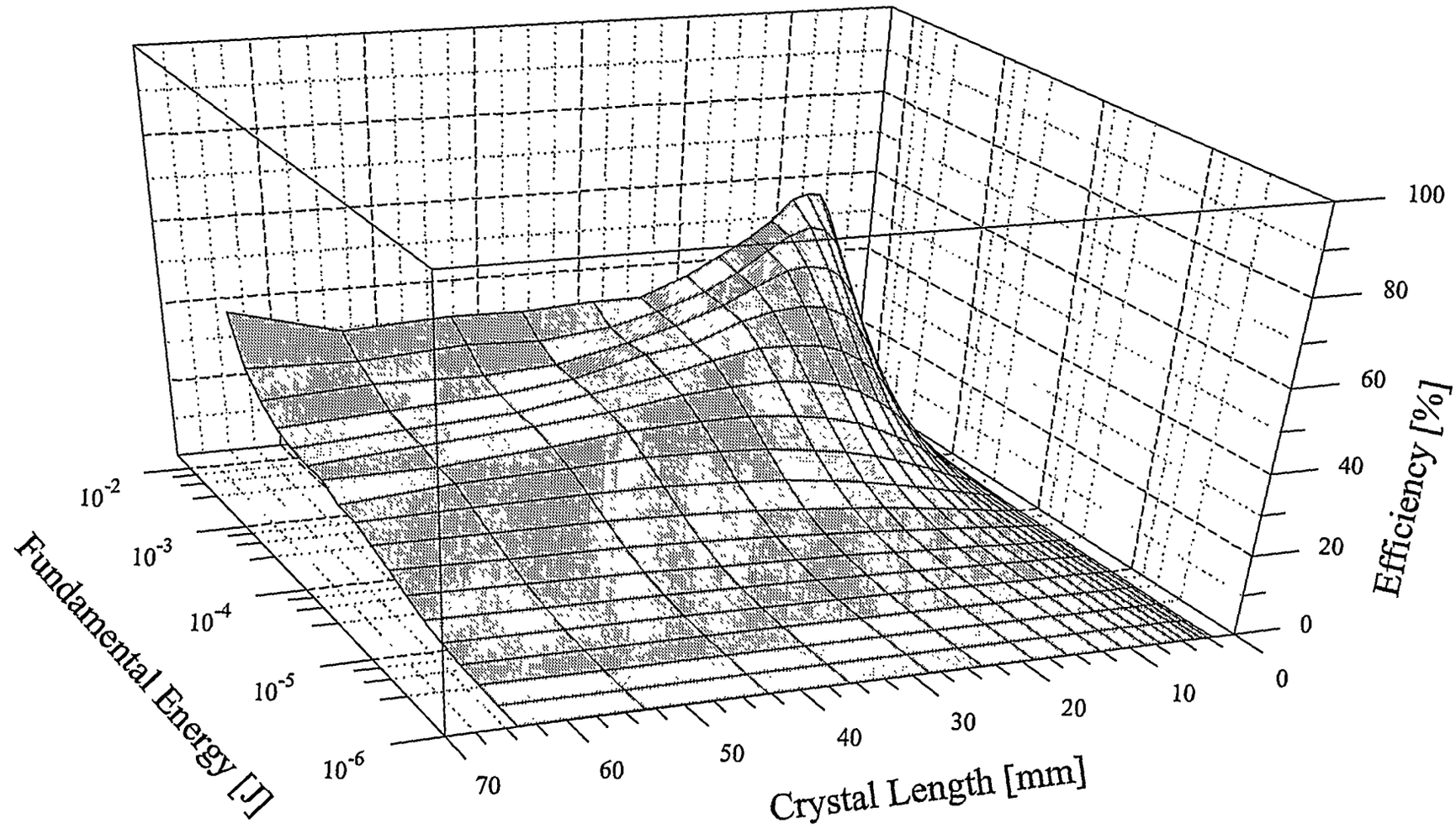
Fundamental Energy [J]
10^-2
10^-3
10^-4
10^-5
10^-6
Crystal Length [mm]
70
60
50
40
30
20
10
0
Efficiency [%]
100
80
60
40
20
0

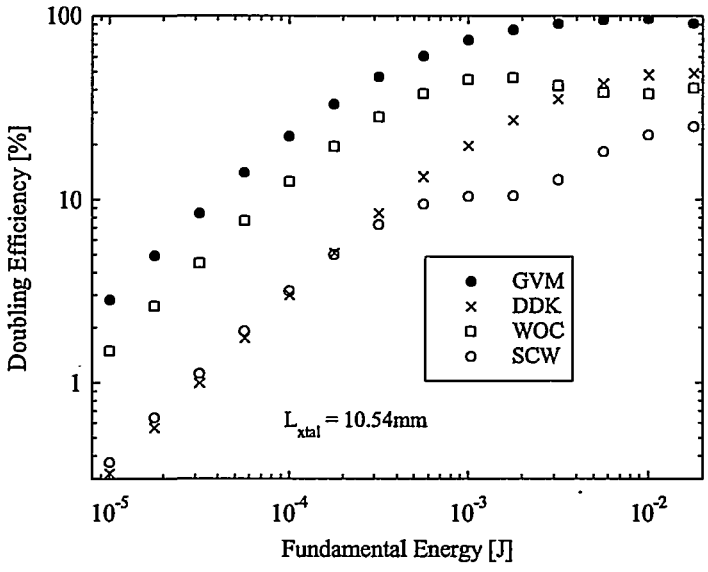
100
10
1
Doubling Efficiency [%]
10^{-5}
10^{-4}
10^{-3}
10^{-2}
Fundamental Energy [J]
GVM
DDK
WOC
SCW
L_{xtal} = 10.54mm

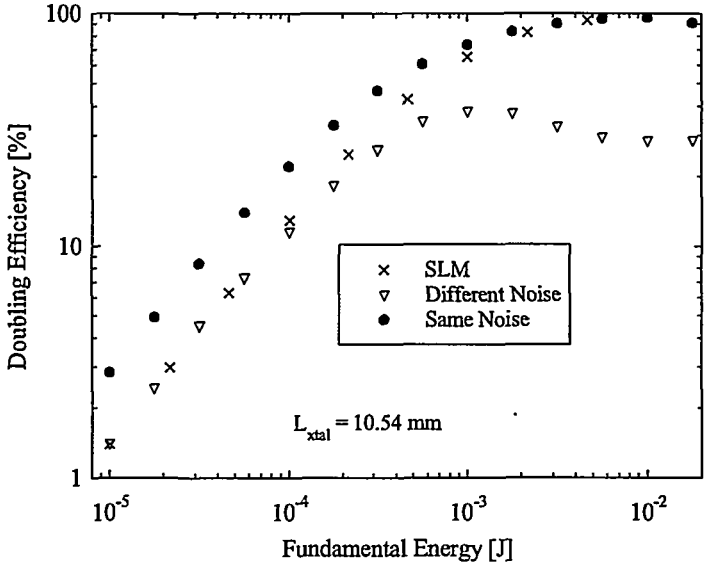
100
10
1
Doubling Efficiency [%]
10^{-5}
10^{-4}
10^{-3}
10^{-2}
Fundamental Energy [J]
SLM
Different Noise
Same Noise
L_{xtal} = 10.54 mm